Biofilm 7 (2024) 100201

Contents lists available at ScienceDirect

Biofilm

journal homepage: www.sciencedirect.com/journal/biofilm

New insights into the antibiofilm activity and mechanism of Mannosylerythritol Lipid-A against *Listeria monocytogenes* EGD-e

Xiayu Liu [b], Siyu Liu [a,b], Yuxi Wang [a], Ying Shi [a], Qihe Chen [a,b,*]

[a] Department of Food Science and Nutrition, Zhejiang University, Hangzhou, 310058, China
[b] Innovation Center of Yangtze River Delta, Zhejiang University, Jiashan, 314100, China

ARTICLE INFO

Keywords:
Mannosylerythritol lipid-A (MEL-A)
L. monocytogenes EGD-e
Antibiofilm
Metabolomics

ABSTRACT

Listeria monocytogenes is one of the leading causative agents of foodborne disease outbreaks worldwide. Herein, the antibiofilm effect and mechanism of Mannosylerythritol Lipid-A against *L. monocytogenes* EGD-e is reported for the first time. MEL-A effectively attenuated biofilm formation while reducing the viability and motility of bacteria within the biofilm in the early stage, and influenced bacterial adhesion by affecting the secretion of extracellular polysaccharides and eDNA. RT-qPCR revealed that MEL-A significantly suppressed the expression of genes involved in flagellar movement and virulence. Untargeted LC-MS metabolomics indicated that MEL-A affected the fluidity and permeability of cell membranes by significantly upregulating unsaturated fatty acids, lipids and glycoside metabolites, and affected protein biosynthesis, nucleotide metabolism and DNA synthesis and repair by significantly downregulating amino acid metabolism and nucleic acid metabolism. These pathways may constitute the key targets of biofilm formation inhibition by MEL-A. Furthermore, MEL-A showed good removal effects on mature biofilms under different temperatures, different materials and milk. Our data indicated that MEL-A could be used as a novel antibiofilm agent to improve food safety. Our study provides new insights into the possible inhibitory mechanism of MEL-A and the response of *L. monocytogenes* EGD-e to MEL-A.

1. Introduction

Listeria monocytogenes is a foodborne pathogen closely associated with human diseases. This facultative anaerobic Gram-positive bacterium is highly tolerant of extreme environments: it can grow at temperatures ranging from −0.4 to 50 °C, pH ranges from 4.1 to 9.6, and high salt concentrations of 10 %–20 % [1]. The 13 serotypes of *L. monocytogenes* have been divided into 4 evolutionary lineages and 63 clonal complexes (CCs) by multilocus sequence typing (MLST) [2]. Serotypes 1/2a and 1/2b are primarily involved in gastrointestinal-related disease outbreaks, and serotype 4b is primarily associated with outbreaks of listeriosis associated with sepsis, central nervous system damage, and fetal infections [1]. According to the Centers for Disease Control and Prevention (CDC) online data tool (National Outbreak Reporting System, NORS), as many as 78 outbreaks of foodborne illnesses caused by *L. monocytogenes* occurred between 2010 and 2020, resulting in a total of 788 illnesses, including 692 hospitalizations and 128 deaths (https://wwwn.cdc.gov/norsdashboard/). Although cases of listeriosis are not as common as other foodborne diseases, the associated high mortality rate (20–30 %) makes it an important foodborne disease that places a severe burden on the lives and health of people worldwide.

Various external and internal factors affect the formation of *L. monocytogenes* biofilm [3]. The amount and microstructure of biofilm significantly depends on environmental parameters such as temperature, humidity, nutrient content, osmotic pressure, culture method, surface properties of the material, etc. [3]. The relevant internal factors mainly include strain serotype, EPS, quorum sensing (QS) system, etc. [4]. Nonetheless, the pathogenicity, resilience and drug resistance of *L. monocytogenes* increase significantly with the formation of biofilm, which leads to its continuous transmission and cross-contamination in the food processing environment, potentially triggering outbreaks of foodborne diseases and significant economic losses in the food industry [3]. Currently, antibiotics constitute the most effective treatment option for biofilm-associated bacterial infections; however, bacteria living in biofilms exhibit increasingly higher patterns of adaptive resistance to antibiotics and other antimicrobial agents compared to planktonic bacteria [5], and treatment of biofilm-associated acute and chronic infections requires a tenfold to thousandfold increase in antibiotic doses [6]. This prompts an urgent need to discover new antibacterial agents that can effectively prevent and control biofilm formation and

* Corresponding author. Yuhangtang Rd.866, Department of Food Science and Nutrition, Zhejiang University, Hangzhou, 310058, China.
E-mail address: Chenqh@zju.edu.cn (Q. Chen).

https://doi.org/10.1016/j.biofilm.2024.100201
Received 3 January 2024; Received in revised form 28 April 2024; Accepted 9 May 2024
Available online 11 May 2024

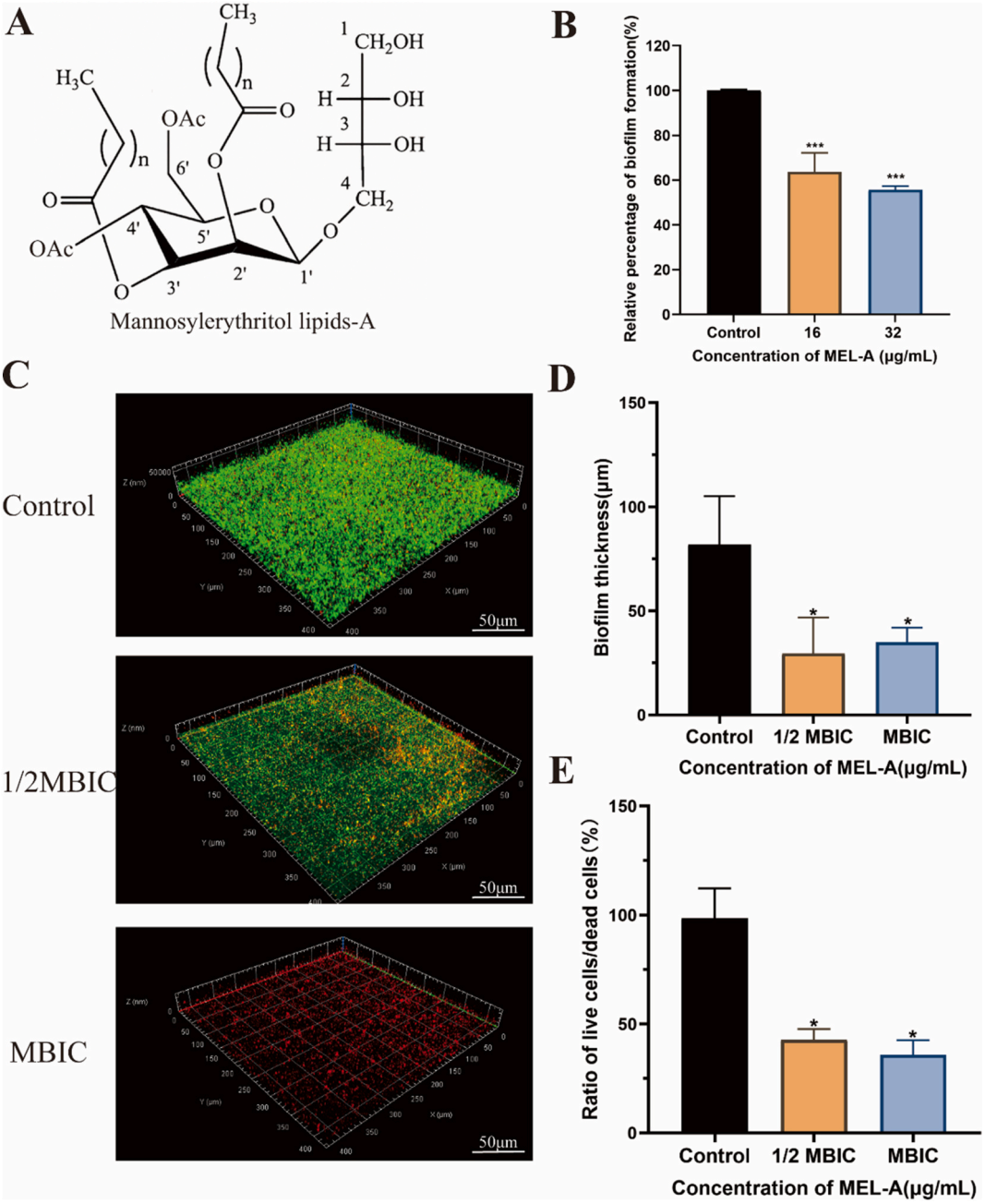

Fig. 1. Inhibitory effect of MEL-A on the biofilm formation of *L. monocytogenes* EGD-e. A. Chemical structure of MEL-A. B. Effect of MEL-A on the biofilm formation of *L. monocytogenes* EGD-e. C. CLSM images of *L. monocytogenes* EGD-e biofilms. D. Biofilm thickness of different groups. E. Live/dead cell ratio of different groups.

development.

Mannosylerythritol lipids (MELs), as biosurfactants with amphiphilic properties, contain hydrophilic groups dominated by 4-O-β-D-mannose-erythritol and hydrophobic groups dominated by fatty acid chains [7]. As shown in Fig. 1A, MELs can be divided into four different configurations according to the degree of acetylation: MEL-A is diacetylated at sites C4 and C6, MEL-B and MEL-C are monoacetylated at sites C6 and C4, respectively, whereas MEL-D has no acetyl group [8–10]. This structural diversity endows MELs with unique biological properties, including high biodegradability, environmental compatibility, antioxidant, antitumor, antimicrobial activity, skin moisturizing, and enzyme activation/inhibition effect, etc. [11]. Fukuoka et al. [12] found that both MEL-A and MEL-B possess strong antimicrobial activity, especially against Gram-positive bacteria, and the antimicrobial activity of MELs is closely related to the level of damage caused to cell membranes. In addition, MEL-A and MEL-B have lower MIC values against Gram-positive bacteria than other glycolipid biosurfactants, such as sucrose decanoate (SE10), sorbitan monolaurate (Span20) and rhamnolipid (RL) [13,14]. Studies have shown that the amount of organic acids such as benzoic acid and sorbic acid needs to be a minimum of 1 % weight percentage to effectively inhibit the biofilm formation of *L. monocytogenes*. This amount for natural extracts such as curcumin and garlic extract is 2–5% weight percentage, and that for nisin is 4–5% weight percentage [15]. MEL-A is an antibacterial agent with great potential; further research on its antibacterial activity will greatly promote the development of novel biological antibacterial agents and may solve the global antibiotic resistance crisis. Despite this promising avenue, there have been few reports on the antibiofilm activity of MEL-A against *L. monocytogenes* EGD-e, and the relevant mechanism remains unkonw. This work, reveals the antibiofilm activity of MEL-A as a novel

antibiofilm agent against *L. monocytogenes* EGD-e and elucidates its mechanism of action by investigating its effects on the global metabolomic alteration and related gene expression.

2. Materials and methods

2.1. Bacterial strains and chemicals

L. monocytogenes EGD-e was purchased from the American Type Culture Collection (ATCC BAA-679, serovar 1/2a) and MEL-A (80 % purity) was produced in our lab from *Pseudozyma aphidis* DSM 70725 by the previously reported method. (L. [16]).

2.2. Screening of L. monocytogenes EGD-e biofilm formation conditions

L. monocytogenes EGD-e was inoculated into BHI broth, cultured overnight (37 °C, 180 rpm), and then diluted in Phosphate Buffered Saline (PBS) to $OD_{600} = 0.1$. Next, 200 μL diluted cultures were absorbed and inoculated into 24-well plates containing four different media (TSB, MEM, TSBg (TSB + 1 % glucose) and BHI), and cultured at 37 °C for 4 h,6 h,12 h,24 h,36 h,48 h,60 h,72 h and 96 h. All biofilm samples were measured by crystal violet staining [17] and observed through optical microscope. Firstly, the supernatant of the samples was removed and washed 3 × with PBS. Subsequently, the well plates were dried in an oven (50–60 °C) for 15 min, and then 1 mL of 1 % (M/V) crystal violet was added for 30 min of staining. Afterwards, the crystal violet was aspirated and washed 3 times with PBS, and the holes were dried in the oven for 15 min. Then 1 mL of glacial acetic acid (33 %, V/V) was added, followed by placing in the incubator at 37 °C for 40 min for dissolution. Finally, the OD_{595nm} value of each group of samples was determined by a microplate reader (Thermo Fisher Scientific, USA).

2.3. Determination of minimum biofilm inhibitory concentration (MBIC) and minimum biofilm eradication concentration (MBEC)

Bacterial solution was prepared as described above. MEL-A continuously diluted with TSB broth (4, 8, 16, 32, 64, 128, 256 and 512 μg/mL) was added to the experimental group, while TSB broth without MEL-A was used as the control. After incubation at 37 °C for 2 days, 20 μL of MTT solution (5.0 mg/mL) was added to each well for 4 h. Subsequently, the wells were washed with PBS, and the $OD_{570\ nm}$ was determined by an enzyme marker after decolorization. The minimum concentration with no significant change in OD value compared with the control group was set as MBIC [18,19]. The MBEC was determined as follows: firstly, mature biofilm was cultured in the wells, the planktonic bacteria were then washed with PBS, followed by the addition of MEL-A at the same concentration as above and incubation at 37 °C for 24 h. Finally, the OD_{570nm} was measured after staining and decoloration with MTT solution as above, and the minimum concentration that showed no significant change in the OD value compared with that of the blank group was designated as the MBEC value.

2.4. Determination of bacterial viability in biofilms

The Cell Counting KIT-8 (CCK-8) was used to determine the activity of bacteria in biofilms [20,21]. Itis a rapid and highly sensitive assay for bacterial activity by applying a novel water-soluble monosodium tetrazole salt 2-(2-methoxy-4-nitrophenyl)-3-(4-nitrophenyl)-5-(2,4-disulfophenyl)-2H-tetrazole (T. [22]). This tetrazolium salt can be reduced to an orange-colored formazan by bacterial dehydrogenase in the presence of electron carriers, and the amount of formazan produced is proportional to the bacterial activity. For the same bacteria, there is a linear relationship between the shade of color and bacterial activity. The inoculation of the bacterial solution was performed as described in Section 2.2, and MEL-A at concentrations of 1/4 MBIC and 1/2 MBIC was added in the experimental group, while the control group was supplemented without MEL-A. After incubation at 37 °C for 6 h and 24 h, the bacterial activity was determined according to the instructions of the CCK-8 kit. The survival rate of *L. monocytogenes* EGD-e in the biofilm was calculated according to the following formula [20,21]:

$$S(\%) = \frac{M(OD_{450}) - M(OD_{650})}{C(OD_{450}) - C(OD_{650})} \times 100\%$$

S: survival rate; M: MEL-A treated; C: control.

2.5. Motility assessment

Motility was determined according to the method provided by Rashid et al. [23] with slight modifications. Firstly, BHI plates containing 0.3 % agar were prepared, then MEL-A at concentrations of 1/4 MBIC and 1/2 MBIC was added to the experimental group. After cooling the plates to room temperature, 1 μL of bacterial solution was spiked into the middle of the plate, which was incubated overnight followed by determining the diameter of the colonies.

2.6. Examination by confocal laser scanning microscope (CLSM)

Bacterial solution prepared as described above was inoculated into confocal petri dishes. The experimental group was added with MEL-A at concentrations of 1/4 MBIC and 1/2 MBIC, while the control group received no MEL-A. After incubation at 37 °C for 48 h, the supernatant was removed, and after 3 × PBS cleaning, SYTO9/PI fluorescent dye was added. After 30 min incubation in darkness, the biofilm formation of each group was assessed by laser confocal microscopy (GeminiSEM300, ZEISS, German). The obtained data were analyzed by Zen and Image J software.

2.7. Determination of extracellular polymer content

The determination of exopolysaccharides was carried out according to the method provided by Upadhyay et al. [24] after slight modification. The bacterial solution was prepared as described above and inoculated into 24-well plates. MEL-A with concentrations of 1/4 MBIC and 1/2 MBIC was added to the experimental group, while the control group received no MEL-A. After 48 h of culture at 37 °C, the supernant was removed, and after 3 × PBS cleaning, 2 mL 0.01 % (M/V) ruthenium red staining solution (Yeasen, Shanghai, China) was added. This was followed by static culture at 37 °C for 1 h, then the OD_{450nm} value of each group of samples was determined by the microplate reader (Thermo Fisher Scientific, USA).

The extracellular protein and eDNA contents were determined with reference to the method adopted by Zhang et al. [18,25]. Firstly, coverslips were placed in 12-well plates, then MEL-A at concentrations of 1/4 MBIC and 1/2 MBIC was added to the experimental group. After incubation at 37 °C for 48 h, the supernatant was removed, and the coverslips were washed 3 × with PBS before being placed in 50 mL centrifuge tubes filled with 10 mL of PBS. Subsequently, the bacterial suspension was sonicated, then centrifuged (20,000 r/min, 20 min) and filtered through a 0.22 μm filter membrane to obtain the EPS samples. The content of extracellular proteins in the EPS samples was determined using the BCA Protein Concentration Measurement Kit (Yeasen, Shanghai, China), and the content of eDNA was measured using a UV-VIS mini spectrophotometer (Nano-300, Allsheng, China).

2.8. Real-time fluorescence quantitative PCR assay

The overnight culture was adjusted to $OD_{600nm} = 0.1$, and 80 μL of bacterial solution was taken for inoculation into 8 mL of freshly prepared TSB medium. This was incubated at 37 °C until $OD_{600nm} = 0.4$, then added with MEL-A to a final concentration of 1/4 MBIC and 1/2 MBIC, and the incubation was continued for 24 h. Next, the supernatant was removed and the sample was washed 3 × with PBS. Next, RNA was

extracted using the instructions for the MolPure® Bacterial RNA Kit (Yeasen, Shanghai, China), and cDNA was synthesized using the PrimeScript RT Reagent Kit (Takara, Beijing, China). TB Green® Premix Ex Taq™ Kit (Thermo Fisher Scientific, MA, USA) and Applied Biosystems™ QuantStudio™ 3 instrument (Thermo Fisher Scientific, MA, USA) were used for subsequent gene expression analysis. The primer sequences were shown in Table S1. The $2^{-\Delta\Delta Ct}$ method was adopted for further analysis.

2.9. Untargeted metabolomics analysis

(1) Sample preparation: Briefly, 32 μg/mL MEL-A was added to the experimental group, while no MEL-A was added to the control group, with six replicates in each group. When the bacterial culture was complete, the supernatant was removed and washed three times with PBS. The biofilm was obtained with a cell scraper, centrifuged at low temperature, snap-frozen in liquid nitrogen, and stored in a refrigerator at −80 °C until further testing.
(2) Metabolite extraction: The samples were thawed, then 100 μL quantities were added to a 2 mL EP tube with 300 μL of methanol (80 %). The samples were frozen in liquid nitrogen for 5 min, then thawed on ice, vortexed for 30 s, and sonicated for 6 min. The supernatant was centrifuged (5000 rpm, 4 °C) into a new EP tube and lyophilized. A corresponding volume of 10 % methanol solution was added for dissolution, followed by LC-MS injection and analysis.
(3) LC-MS/MS analysis: The samples were analyzed on a Vanquish UHPLC ultra-high performance liquid chromatograph (Thermo Fisher, MA, USA) equipped with a Hypesil Gold column (C18) (Thermo Fisher, MA, USA) at a column temperature of 40 °C and a flow rate of 0.2 mL/min. The mobile phases were 0.1 % formic acid in mobile phase A and methanol in mobile phase B in the positive mode, while they were 5 mM ammonium acetate in mobile phase A and methanol in mobile phase B in the negative mode. The gradient elution program was as follows:

Time	A%	B%
0	98	2
1.5	98	2
3	15	85
10	0	100
10.1	98	2
11	98	2
12	98	2

The Q Exactive™ HF-X mass spectrometer (Thermo Fisher, Germany) was used for mass spectrometry analysis, with the following settings: scan range *m/z* 100–1500; ESI source settings: spray voltage 3.5 kV, sheath gas flow rate 35 psi, auxiliary gas flow rate 10 L/min, ion transfer tube temperature 320 °C, S-lens RF level 60, auxiliary gas heater temperature 350 °C, polarity: positive, negative; data-dependent MS/MS secondary scan. Subsequent data processing, metabolite identification and statistical analysis were completed by Novogene Co., Ltd. (Beijing, China).

2.10. Effect of MEL-A on mature biofilm

Firstly, the bacterial solution was prepared as described in Section 2.2, then inoculated into 24-well plates and cultured at 37 °C for 48 h. The suspended bacterial solution was removed, washed 3 × with PBS, added with 2 mL of MEL-A at concentrations of 0, 1/2 × MBIC, 1 × MBIC, and 2 × MBIC, then incubated at 37 °C for 4 h and subjected to crystalline violet staining, metabolic viability measurements, viable bacterial counts, and fluorescent microscope observations as described above. The eradication activity of MEL-A on mature biofilm in different culture systems was also determined by varying the incubation temperature (4 °C, 25 °C, 37 °C), the culture material (stainless steel, glass, polystyrene) and the medium (milk). The bacterial solution was prepared and inoculated as above, and the length of treatment with MEL-A was 8 h.

2.11. Statistical analysis

At least 3 parallel groups were set up for each set of experiments, and data were presented as mean ± SEM. One-way analysis of variance (ANOVA) and Duncan's multiple range test (DMRT) were used for statistical analysis. All data were considered significant only when $P < 0.05$.

3. Results and discussion

3.1. Inhibitory effect of MEL-A on the biofilm formation of *L. monocytogenes* EGD-e

L. monocytogenes can attach to the surface of various food processing equipment and form biofilm. Once the biofilm has been formed, bacterial survival time can be greatly extended, thus bringing great risks for food safety [24]. Therefore, to deeply understand the biofilm formation characteristics of *L. monocytogenes*, we first explored the conditions for its biofilm formation. As shown in Fig. S1A, the biofilm formation effect of *L. monocytogenes* EGD-e in TSB and TSBg medium was better, and the amount of biofilm was significantly higher than that in MEM and BHI. Microscopic observation also revealed that the biofilms formed in TSB and TSBg were denser (Fig. S1C), hence TSB medium was used for subsequent experiments. From the perspective of biofilm formation time (Fig. S1B), the amount of formed biofilm gradually increased within 0–48 h, reached the maximum value at 48 h, and then gradually decreased.

In order to investigate the inhibitory effect of MEL-A on the biofilm formation of *L. monocytogenes* EGD-e, we firstly determined the MBIC and MBEC values of MEL-A based on the MTT method. As shown in Fig. S2, the MBIC and MBEC values of MEL-A inhibiting biofilm formation were 64 μg/mL and 256 μg/mL, respectively. In our previous study, MEL-A inhibited the growth of *L. monocytogenes* EGD-e in the planktonic state with an MIC value of 32 μg/mL [20], and the significant increase in the MBIC value here could be attributed to the formation of a complex three-dimensional structure of the bacteria and the extracellular polymers in the biofilm [26], which led to a significant increase in bacterial tolerance to the drug.

Next, the effect of MEL-A on the biofilm formation of *L. monocytogenes* EGD-e was determined by crystal violet staining. As shown in Fig. 1B, the biofilm formation of *L. monocytogenes* EGD-e was reduced by 36.3 % and 44.3 % after treatment with 1/4 MBIC (16 μg/mL) and 1/2 MBIC (32 μg/mL) of MEL-A, respectively. To more intuitively observe the effect of MEL-A on biofilm formation, the three-dimensional structure of biofilm was examined by laser confocal microscopy. As shown in Fig. 1C–a dense multilayer biofilm structure was formed in the control group, with a large number of cell aggregates and live cells occupying the main body. On the contrary, in the MEL-A treated group, the colonies were sparse, the aggregation phenomenon was obviously weakened and a large number of dead cells were seen. Biofilm thickness was determined and live-dead cell comparisons were madeby Zen and Image J software, respectively, and the results showed that the biofilm thickness (Fig. 1D) and the proportion of live cells (Fig. 1E) in the MEL-A treatment group were significantly reduced, consistent with the results in Fig. 1C. In summary, the results indicated that MEL-A demonstrated a significant inhibitory effect on biofilm formation, and this effect showed a certain concentration dependence.

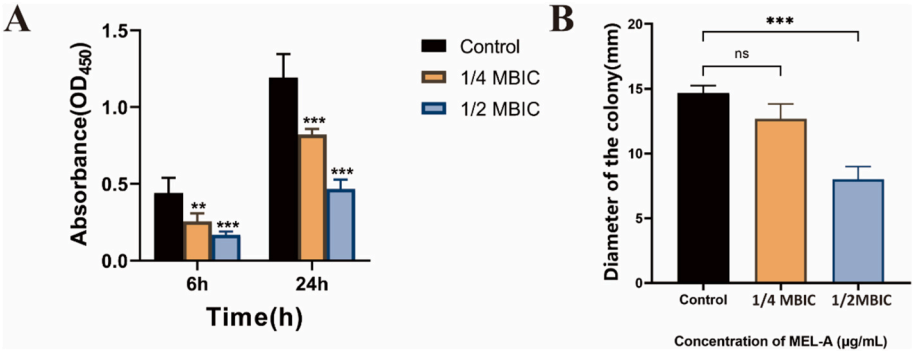

Fig. 2. Effect of MEL-A on the viability (A) and motility (B) of *L. monocytogenes* EGD-e in the biofilm. The symbol *** indicates significant difference, $P < 0.001$.

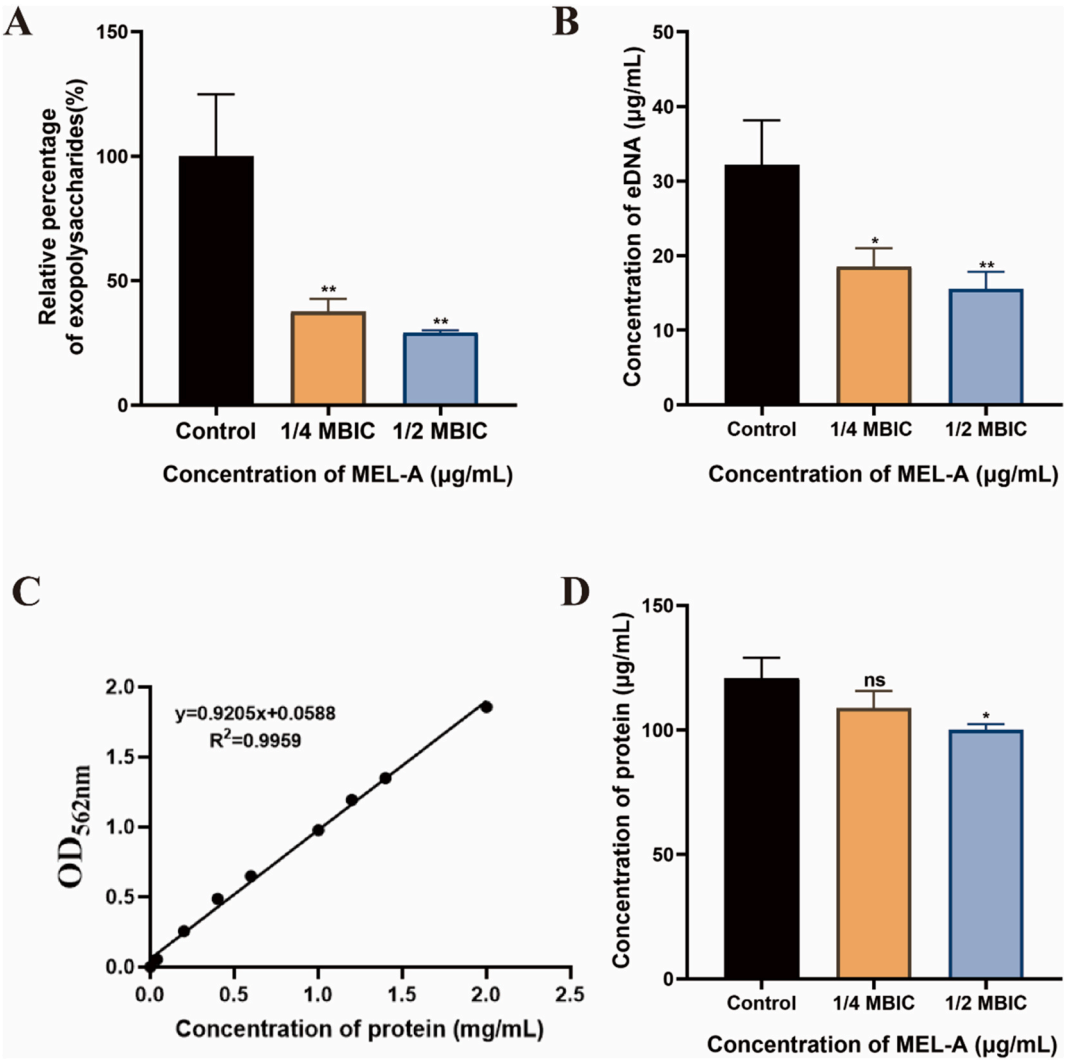

Fig. 3. Effect of MEL-A on the extracellular polymeric substances of *L. monocytogenes* EGD-e. A. Exopolysaccharide content. B. Extracellular eDNA content. C. Standard curve for the extracellular protein assay. D. Extracellular protein content. The symbols * and ** indicate significant difference at $P < 0.05$ and $P < 0.01$, respectively.

3.2. *Effect of MEL-A on the viability and motility of bacteria in biofilm*

As shown in Fig. 2A, after treatment with 1/4 MBIC and 1/2 MBIC MEL-A for 6 and 24 h, bacterial activity decreased by 42 % and 62 % and by 31 % and 61 % respectively, compared with the control group, indicating that MEL-A significantly inhibited the early activity of bacteria in the biofilm. Bacterial activity is closely related to the metabolic ability of bacteria, suggesting that MEL-A may cause damage to the bacterial cell membrane structure in the biofilm and affect this early metabolic activity, which may be one of the key mechanisms of MEL-A inhibiting the biofilm formation. Moreover, research on the bacterial cells in the Viable but nonculturable (VBNC) state has emerged in recent years (J. [27]). As shown in Fig. S5, by comparing the proportion of viable cells and the proportion of culturable cells in the biofilm after

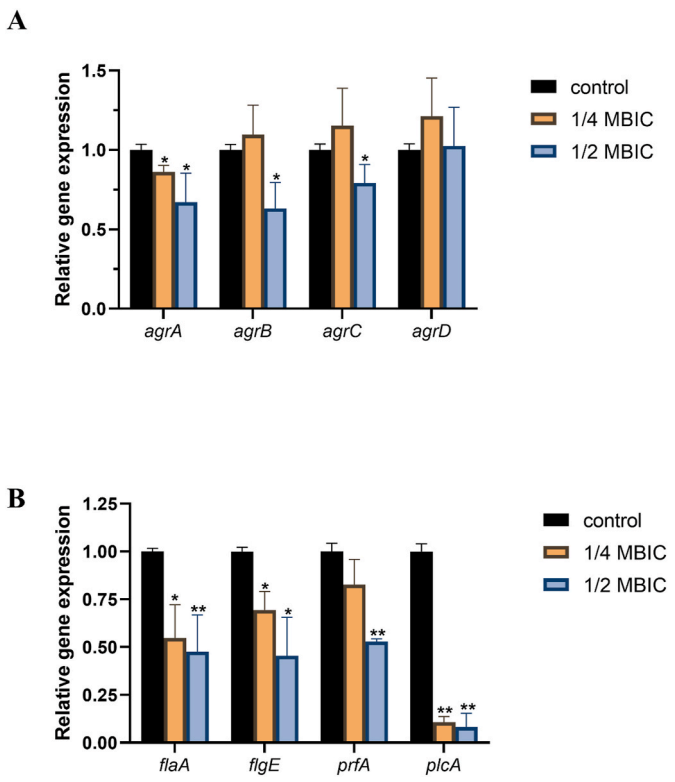

Fig. 4. Effect of MEL-A on the gene expression of *L. monocytogenes* EGD-e. The symbols * and ** indicate significant difference at $P < 0.05$ and $P < 0.01$, respectively.

MEL-A (32 μg/mL) treatment for 48 h, it can be seen that the proportion of viable cells was 42 %, and the number of culturable cells was 13 %, which indicated that MEL-A can kill most bacteria in the biofilm (58 %). However, about 29 % of cells still entered the VBNC state, which deserves our attention. Hence, the effect of MEL-A on the VBNC status of *L. monocytogenes* and its mechanism need to be further studied.

Bacterial motility is also critical for biofilm formation. During reversible adhesion, bacteria attach to the substrate via cell polarization or flagella, followed by longitudinal attachment. As shown in Fig. 2B, compared with the control group, the colony diameter was reduced by 45 % when the concentration of MEL-A reached 1/2 MBIC, while there was no significant effect at 1/4 MBIC. The results indicated that MEL-A could significantly reduce the motility and diffusion range of *L. monocytogenes* EGD-e. Therefore, the effect of MEL-A on the crawling motility of bacteria might be one of the causes of the observed decreased biofilm formation.

3.3. Effect of MEL-A on extracellular polymeric substances (EPS) in biofilm

Extracellular polymeric substances (EPS), together with microbial cells, formthe complex structure of biofilm. EPS are mainly composed of exopolysaccharides, proteins and extracellular DNA (eDNA), which can provide mechanical stability for biofilms by forming a unique three-dimensional spatial structure. Previous studies have shown that EPS can not only immobilize biofilm cells, but also promote strong interactions between them, including intercellular communication, horizontal gene transfer, and the formation of synergistic associations [28]. In addition, EPS contributes to the initial attachment and nutrient capture of bacteria and the integrity of the biofilm structure [29,30].

As shown in Fig. 3A, we measured the exopolysaccharide content after MEL-A treatment by the color reaction of the cationic dye ruthenium red combined with the polysaccharide complex. Compared with the control group, the exopolysaccharide content decreased by 62.4 % and 70.8 % after MEL-A treatment at 1/4 MBIC and 1/2 MBIC, respectively, indicating that MEL-A significantly inhibited the secretion of exopolysaccharide in *L. monocytogenes* EGD-e. MEL-A also resulted in a significant reduction in the eDNA content (Fig. 3B), namely, 42.3 % and 51.6 % after 1/4 MBIC and 1/2 MBIC of MEL-A treatment, respectively.

Furthermore, the extracellular protein content was determined by the BCA protein assay kit. The equation of the protein standard curve was: $y = 0.9205x+0.0588$ ($R^2 = 0.9959$) (Fig. 3C). Based on the standard curve, the protein content of the control group, 1/4 MBIC group and 1/2 MBIC group were 120.8 μg/mL, 108.9 μg/mL and 100.2 μg/mL, respectively. Compared with the control group, the protein content of 1/4 MBIC treatment group and 1/2 MBIC treatment group decreased by 9.9 % and 17.1 %, respectively. In conclusion, the degree of influence MEL-A exerts on EPS was in the descending order of exopolysaccharides > eDNA > protein. Therefore, via the secretion of extracellular polysaccharide, the adhesion of bacteria is affected, which may be one of the key mechanisms of MEL-A inhibiting biofilm formation.

3.4. Molecular mechanism of MEL-A regulation on biofilm

In order to comprehensively investigate the molecular mechanism of MEL-A inhibiting biofilm formation, the effects of MEL-A on the expression of quorum sensing-related genes (*agrA*, *agrB*, *agrC*, *agrD*), motility-related genes (*flaA*, *flgE*, *flgG*, *motB*) and virulence-related genes (*inlA*, *inlB*, *prfA*, *plcA*) were determined by RT-qPCR analysis. As shown in Fig. 4B, when the concentration of MEL-A reached 1/2 MBIC, motility-related genes (*flaA*, *flgE*) and virulence-related genes (*prfA*, *plcA*) were down regulated by more than twofold. In particular, the gene *plcA* was down-regulated by 12-fold. Meanwhile, quorum sensing-related genes (*agrA*, *agrB*, *agrC*) were only slightly downregulated (less than 2-fold) (Fig. 4A).

Both *flaA* and *flgE* are flagellar motility-related genes. Flagellate-mediated motility is crucial for biofilm formation, and flagella are also closely associated with surface adhesin in the surface attachment of *L. monocytogenes* (Y. [31]). Studies have shown that the deletion of genes *flaA* [32] and *flgE* (F. [33]) both lead to defects in bacterial biofilm formation. Thus, significantly downregulating these motility-related genes by MEL-A diminishes flagellar motility, ultimately leading to impaired biofilm formation, which is also consistent with the motility assay results described above. The virulence-related genes *prfA* and *plcA* were also significantly down-regulated. As a key transcriptional activator, PrfA can positively regulate virulence genes in *L. monocytogenes* to mediate the transition from extracellular, flagellum-driven cells to intracellular pathogens [32]. PrfA can promote the formation of flagellin and its deletion also leads to the weakening of biofilm formation ability. Gene *plcA* is located upstream of *prfA* and is a key promoter driving the expression of prfA, however, the deletion of *plcA* alone does not directly lead to a decrease in the biofilm formation ability of *L. monocytogenes* [32]. Therefore, MEL-A may block the expression of PrfA by inhibiting *plcA*, thereby affecting the formation of flagellin. In conclusion, we established that MEL-A can inhibit the formation of *L. monocytogenes* EGD-e biofilm by controlling the expression of flagellar motility genes and virulence genes.

3.5. Effect of MEL-A on global metabolomics

3.5.1. Multidimensional statistical analysis of metabolomic data

Metabolomics has been widely used to reveal the properties of food-associated microorganisms and the antibacterial mechanisms (Y. [34]; N. [35]). The effects of MEL-A on *L. monocytogene* biofilm formation were further investigated based on untargeted LC-MS/MS analysis. As shown in Fig. 5, principal component (PCA) analysis was employed to observe the overall distribution trend between the two groups of samples. Replicates of the same groups were significantly clustered together between the experimental group (group M) and the control group (group

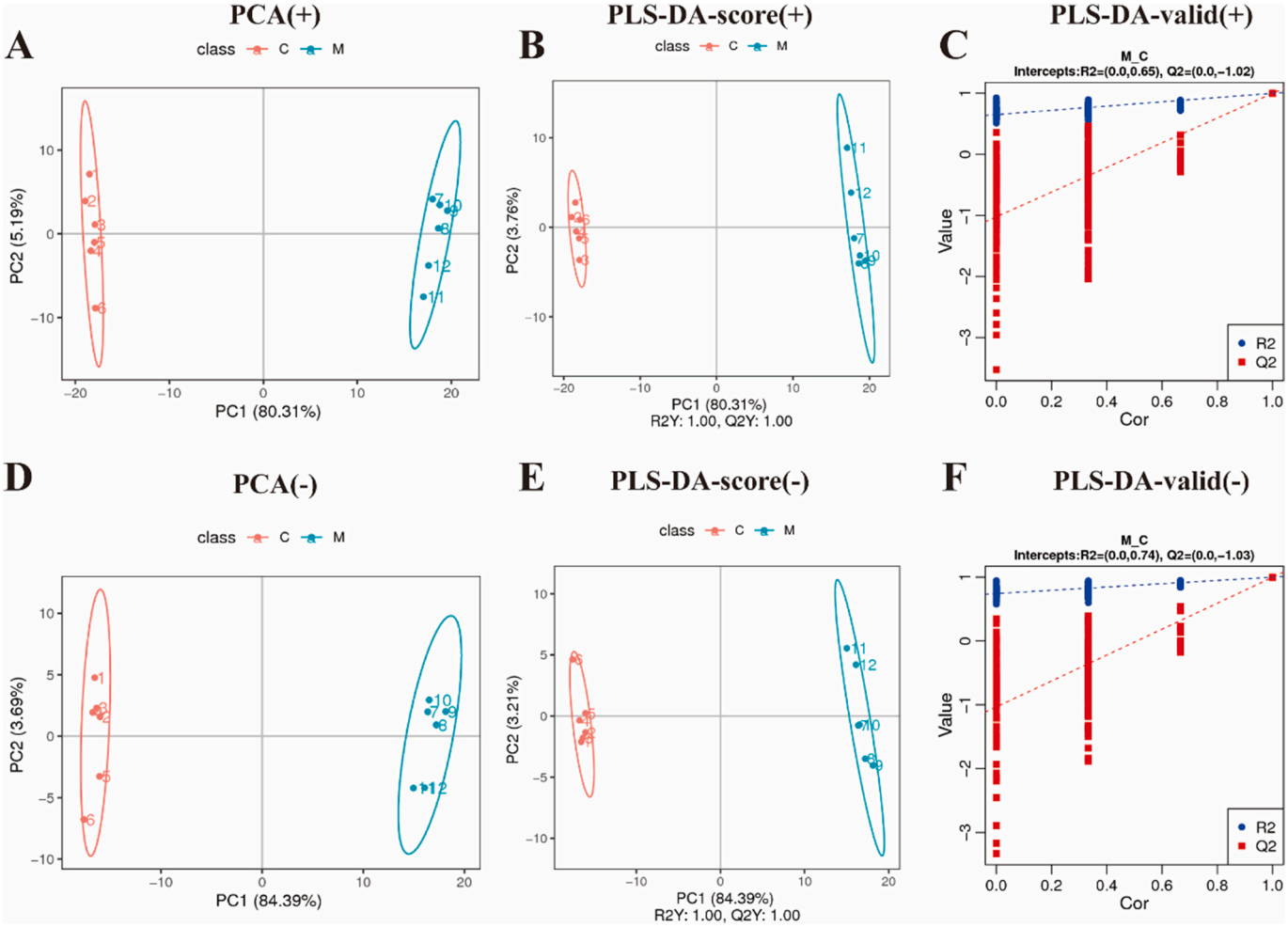

Fig. 5. Multivariate statistical analysis of the metabolomics profile under positive and negative ion mode. PCA score plot of control (without MEL-A) and sample (with MEL-A) under positive (A) and negative (D) ion mode. PLS-DA score plot of the control and sample groups, represented by red and blue, respectively, under positive (B) and negative (E) ion mode. (C) and (F) are PLS-DA sequencing test diagrams for the comparison of positive and negative ion samples, respectively. (For interpretation of the references to color in this figure legend, the reader is referred to the Web version of this article.)

C), while different groups were significantly separated, indicating good reproducibility and sufficient separation resolution in revealing the effect of MEL-A addition. By conducting Partial Least Squares Discrimination Analysis (PLS-DA), it could also be seen that R2 and Q2 were equal to 1 (Fig. 5B–E), indicating the stability and reliability of the model. Moreover, R2 data were larger than Q2 data and the intercept between Q2 regression line and Y-axis was less than 0 (Fig. 5C–F), indicating the high accuracy of model construction.

3.5.2. *Identification of differential metabolites*

As shown in Fig. 6A and B, the screening of differential metabolites was performed according to the criteria of VIP >1.0, FC > 2 or FC < 0.5 and P-value <0.001. A total of 302 metabolites of the positive ion pattern were significantly different in the M vs C comparator group, of which 73 metabolites were upregulated and 229 metabolites were downregulated. A total of 255 metabolites of the negative ion pattern were significantly different, of which 46 metabolites were upregulated and 209 metabolites were downregulated. Cluster analysis showed that the relative abundance of metabolites in the experimental group was significantly different from that of the control group (Fig. 6C and D).

As shown in Table 1, MEL-A resulted in the significant up-regulation of metabolites related to fatty acids and glycerol and in the significant downregulation of metabolites related to amino acids and purine pyrimidines. Fatty acids, either free or as part of complex lipids, play a number of key roles in metabolism, such as energy storage and transportation, forming essential components of membranes, and as regulators of genes. MEL-A treatment resulted in a significant upregulation of various unsaturated fatty acids (UFAs) such as arachidonic acid (16(R)-HETE, 5-OxoETE), palmitoleic acid, linoleic acid and elaidic acid. Previous studies have shown that UFAs are essential for the maintenance of cell membrane fluidity [36]. Therefore, MEL-A may affect the fluidity and permeability of cell membranes. Sphingosine kinase (SPK) is the most significantly upregulated positive ion metabolite after MEL-A treatment, and its catalytic product sphingosine 1-phosphate (S1P) is also an important active lipid molecule. Several studies have shown that SPK also has pro-growth and anti-apoptotic effects [37]. Therefore, the significant upregulation of SPK may be a self-protection mechanism of bacteria under MEL-A treatment. In our study, the most significantly upregulated negative ion metabolite was DGMG (18:2), which is a glycoside and an important component of the cell membrane complex.

Furthermore, complex correlations were found between different metabolites (Fig. S3). Among the down-regulated metabolites, the most significant ones were amino acids and their derivatives, such as threonine, proline, alanine-valine, γ-glutamine-leucine, N-acetylornithine, N-lactoylphenylalanine and γ-aminobutyric acid (GABA), and their downregulation rate was more than 50 times. Amino acids serve as important structural units of proteins. The results indicated that MEL-A significantly affected protein biosynthesis during *L. monocytogenes* EGD-e biofilm formation. Another important category is nucleic acid

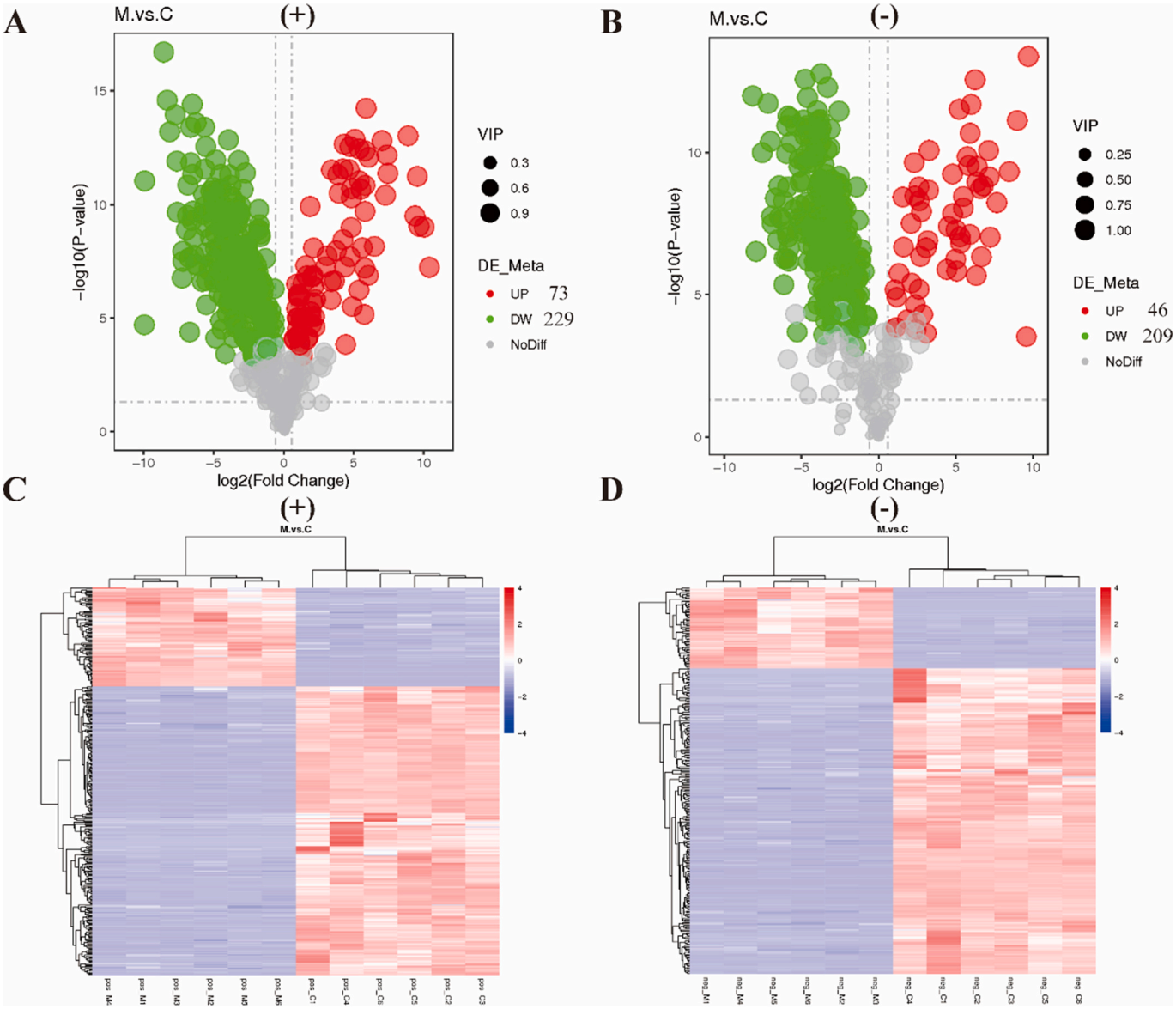

Fig. 6. Identification of differential metabolites under positive and negative ion mode. (A) and (B) are volcanic maps of differential metabolites of positive and negative ion samples, respectively. (C) and (D) are heatmaps of the clustering analysis of differential metabolites in positive and negative ion samples, respectively.

metabolism, where a variety of metabolites related to nucleic acid metabolism, such as purines, pyrimidines, and adenosine, were significantly downregulated (Table 1), suggesting that MEL-A may also affect nucleotide metabolism as well as DNA synthesis and repair in bacteria. In addition, both NAD^+ and NADH were significantly downregulated, with NADPH being the most significantly downregulated negative ion metabolite, with a downregulation factor of up to 288 times. NAD^+ and NADH constitute a redox pair and play a pivotal role in cellular metabolism as cofactors of many dehydrogenases. In addition to being closely associated with glycolysis and the tricarboxylic acid cycle (TCA), NAD^+ and NADH perform other functions in cell signaling pathways, including regulating redox dependent proteins (such as transcription factors), redox dependent signaling (such as Ca^{2+} signaling), and protein activity due to nucleotide availability [38].

As shown in Fig. 7A, the pathway enrichment analysis of altered metabolites indicates that the metabolic pathway was the only significantly enriched KEGG pathway ($P < 0.05$). From the enrichment analysis pathway diagram (Fig. 7B), it could be seen that most downregulated metabolites were concentrated in the two pathways of Amino acid metabolism and Nucleotide metabolism. Theseresults reveal that the effect of MEL-A on amino acid metabolites and nucleic acid metabolites at the metabolic level may be an important reason for its inhibitory effect of *L. monocytogenes* EGD-e on biofilm formation. Our previous transcriptomics-based findings also suggest that MEL-A directly affects carbohydrate utilization and amino acid biosynthesis, and reduces cell membrane bioactivity and permeability by interfering with ABC transporters [20]. This finding is consistent with our metabolomics results and further suggests that MEL-A inhibits *L. monocytogenes* EGD-e biofilm formation by influencing cell membrane fluidity and permeability, protein biosynthesis, nucleotide metabolism, and DNA synthesis and repair.

3.5.3. *Effect of MEL-A on mature biofilms of L. monocytogenes EGD-e*

As a foodborne pathogen, *L. monocytogenes* can attach to various food contact surfaces such as stainless steel, polystyrene, rubber, and glass, leading to the formation of biofilms [39]. Once a mature biofilm is formed, the resistance of the constituting microorganisms to antimicrobial agents and stress will be significantly enhanced, which can easily lead to food contamination and serious health problems. Therefore, we further assessed the biofilm eradication activity of MEL-A on

Table 1
Alteration of representative metabolites in *L. monocytogenes* EGD-e upon MEL-A treatment.

Function	Compound name	VIP value	P value	Fold change	Formula	Molecular weight	Up/dn	ESI
Fatty acid metabolism	Octadec-9-ynoic acid	1.11	5.78E-12	744.74	C18H32O2	262.23	up	+
	16(R)-HETE	1.11	9.86E-10	1048.87	C20H32O3	342.21	up	+
	5-OxoETE	1.11	6.66E-13	166.06	C20H30O3	318.22	up	+
	10-Undecenoic acid	1.12	8.41E-13	66.63	C11H20O2	184.15	up	+
	Palmitoleic Acid	1.11	2.01E-10	55.81	C16H30O2	276.21	up	+
	Heptadecanoic Acid	1.09	6.85E-06	53.82	C17H34O2	292.24	up	+
	Linoleic Acid	1.09	5.78E-09	203.15	C18H32O2	280.24	up	–
	Elaidic acid	1.09	2.77E-13	76.44	C18H34O2	282.26	up	–
Phospholipid metabolism	SPK	1.11	5.81E-08	1346.85	C14H26N4O5	352.17	up	+
	N-Acetyl-α-D-Glucosamine 1-phosphate	1.09	1.14E-11	0.02	C8H16NO9P	265.08	dn	–
Glycerol metabolism	2-Linoleoyl glycerol	1.11	9.00E-10	809.41	C21H38O4	336.26	up	+
	DGMG (18:2)	1.09	4.16E-14	836.15	C33H58O14	678.38	up	–
Antibacterial agents	Tanespimycin	1.12	3.18E-10	660.34	C31H43N3O8	626.33	up	+
	Benzoic acid	1.10	1.33E-07	65.63	C22H30O3	324.20	up	+
Purine, pyrimidine and derivative	NAD^+	1.12	3.88E-15	0.011	C21H27N7O14P2	663.11	dn	+
	NADH	1.09	1.02E-12	0.003	C21H27N7O14P2	663.11	dn	–
Amino acid and derivative	Ala-Val	1.11	2.19E-10	0.005	C8H16N2O3	188.12	dn	+
	Ala-Leu	1.08	5.45E-07	0.014	C9H18N2O3	202.13	dn	–
	Glycyl-L-leucine	1.08	1.49E-09	0.011	C8H16N2O3	188.12	dn	–
	N-lactoyl-phenylalanine	1.08	1.17E-07	0.011	C12H15NO4	237.10	dn	–
	Prolylleucine	1.08	4.06E-09	0.010	C11H20N2O3	228.15	dn	–
	Thr-Leu	1.08	3.20E-08	0.008	C10H20N2O4	232.14	dn	–
	N-Acetylornithine	1.08	1.75E-08	0.008	C7H14N2O3	174.10	dn	–
	GABA	1.11	4.01E-14	0.010	C4H9NO2	103.06	dn	+
	Gamma-Glutamyltyrosine	1.08	3.03E-07	0.004	C14H18N2O6	310.12	dn	–
	L-Alanyl-L-proline	1.12	1.40E-11	0.009	C8H14N2O3	186.10	dn	+
	Leucylproline	1.11	3.16E-08	0.007	C11H20N2O3	228.15	dn	+
	GABA	1.11	4.01E-14	0.010	C4H9NO2	103.06	dn	+
Nucleotide metabolism	Inosine	1.03	9.08E-05	0.126	C10H12N4O5	268.08	dn	–
	Thymidine 5′-monophosphate	1.08	4.56E-09	0.125	C10H15N2O8P	322.06	dn	–
	Thymine	1.09	5.14E-13	0.100	C5H6N2O2	126.04	dn	–
	Purine	1.07	8.88E-06	0.086	C5H4N4	120.04	dn	–
	Uridine	1.06	1.39E-06	0.058	C9H12N2O6	244.07	dn	–
	Guanosine	1.08	2.67E-11	0.047	C10H13N5O5	283.09	dn	–
	Adenosine	1.11	4.07E-12	0.151	C10H13N5O4	267.10	dn	+
	Uracil	1.11	7.00E-10	0.101	C4H4N2O2	112.03	dn	+
	Xanthine	1.08	3.10E-05	0.047	C5H4N4O2	152.03	dn	+

Fig. 7. KEGG enrichment analysis of differential metabolites. A. Bubble plot of KEGG enrichment analysis of differential metabolites. B. KEGG enrichment pathway diagram of differential metabolites.

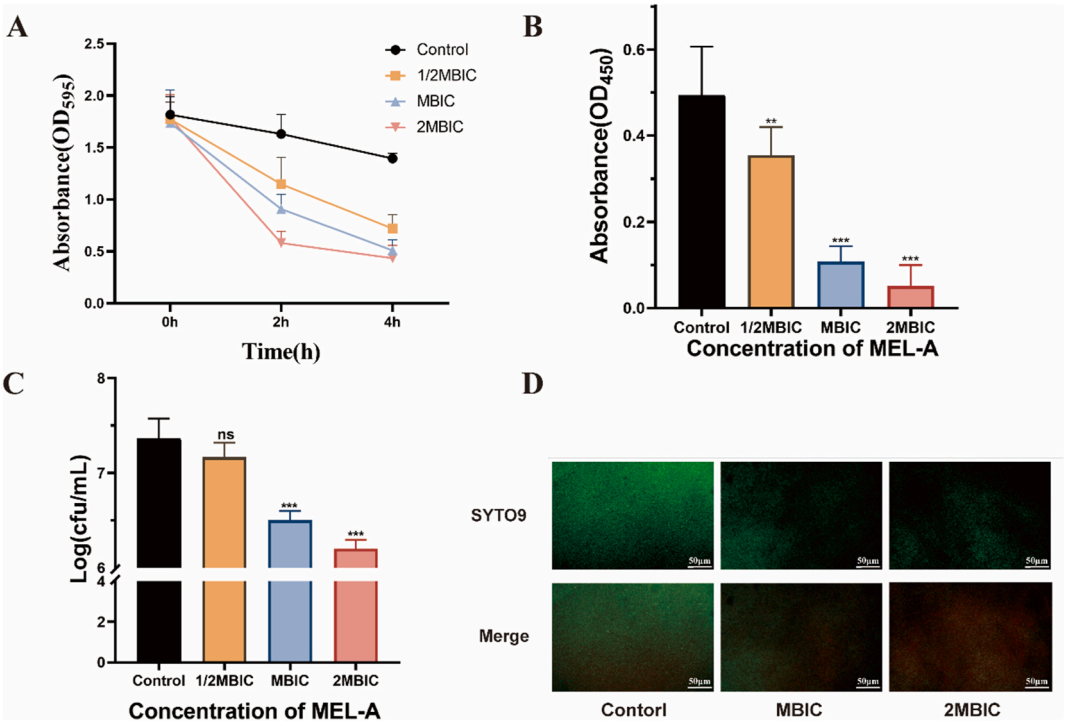

Fig. 8. Biofilm eradication activity of MEL-A. Eradication effect of MEL-A on *L. monocytogenes* EGD-e biofilm (A) and on the activity (B) and number (C) of bacteria in the biofilm. (D) Fluorescence microscopic images after treatment with different concentrations of MEL-A.

L. monocytogenes EGD-e.

After 1/2 MBIC, MBIC and 2 MBIC of MEL-A treatment for 4 h, compared with the control group, the amount of biofilm formed (Fig. 8A) decreased by 48.4 %, 63.6 % and 69 %, respectively, the bacterial activity (Fig. 8B) in the biofilm decreased by 28.1 %, 78.2 % and 89.6 %, the number of bacteria (Fig. 8C) decreased by 2.7 %, 11.8 % and 15.8 %, respectively. These findings indicated that MEL-A had a good biofilm eradication activity and could significantly reduce the activity and abundance of bacteria in the biofilm. Fluorescence microscopy images (Fig. 8D) further visualized this result; the biofilm structure in the MEL-A-treated group became significantly thinner and looser and the number of viable bacteria was significantly reduced compared with the control group. Moreover, the high biofilm eradication activity of MEL-A was further demonstrated by the results of crystal violet staining of MEL-A at different temperatures (4 °C, 25 °C, 37 °C), different materials (stainless steel, glass, and polystyrene), and in the milk system (Fig. S4). The above findings demonstrate that MEL-A can be used as a potential biofilm scavenger in the food industry.

4. Conclusion

In this study, the antibiofilm effect of a novel biosurfactant MEL-A on *L. monocytogenes* EGD-e was investigated for the first time, along with physiological characterization, real-time qPCR analysis and the untargeted LC-MS metabolomic approach to explore the underlying mechanisms. Physiological characterization confirmed that MEL-A significantly inhibited the formation of *L. monocytogenes* EGD-e biofilm and caused the impairment of early bacterial viability, motility and extracellular polymer secretion within the biofilm. MEL-A also significantly suppressed the expression of flagellar motility-related genes and virulence genes. The results of non-targeted metabolomics analysis indicated that MEL-A significantly upregulated unsaturated fatty acids, lipids and glycoside metabolites to affect cell membrane fluidity and permeability, and it significantly downregulated amino acid metabolism and nucleic acid metabolism to affect protein biosynthesis, nucleotide metabolism and DNA synthesis and repair, which may be the key mechanisms behind the inhibitory effect of MEL-A on biofilm formation. Furthermore, significant eradication activity of MEL-A on mature biofilms at different temperatures, materials and the milk system were observed, which strongly suggested that MEL-A could be used as a novel effective antibiofilm agent against foodborne pathogens in the food industry. Our data provides new insights into the possible underlying the multi-target antibiofilm mechanism of MEL-A and improves our comprehension of the response of *L. monocytogenes* EGD-e to MEL-A. However, only one strain of *L. monocytogenes* was used in this study, so the relevant conclusions may not be applicable to other strains or species. Thus, further studies should be carried out on other *Listeria* strains (such as *L.iuanuii* and *L.innocua*).

Funding

This work was supported by the Project funded by China Postdoctoral Science Foundation [2023TQ0281, 2023M743057].

CRediT authorship contribution statement

Xiayu Liu: Writing – review & editing, Writing – original draft, Visualization, Supervision, Resources, Methodology, Investigation, Funding acquisition, Data curation, Conceptualization. **Siyu Liu:** Software, Investigation, Formal analysis, Conceptualization. **Yuxi Wang:** Validation, Investigation, Conceptualization. **Ying Shi:** Visualization, Validation, Software, Resources, Investigation, Formal analysis, Conceptualization. **Qihe Chen:** Writing – review & editing, Validation, Project administration, Methodology, Formal analysis, Conceptualization.

Declaration of competing interest

The authors declare no conflict of interest.

Data availability

Data will be made available on request.

Appendix A. Supplementary data

Supplementary data to this article can be found online at https://doi.org/10.1016/j.bioflm.2024.100201.

References

[1] Thakur M, Asrani RK, Patial V. Chapter 6 - *Listeria monocytogenes*: a food-borne pathogen. In: Holban AM, Grumezescu AM, editors. Foodborne diseases. Academic Press; 2018. p. 157–92.

[2] Radoshevich L, Cossart P. *Listeria monocytogenes*: towards a complete picture of its physiology and pathogenesis. Nat Rev Microbiol 2018;16(1):32–46. https://doi.org/10.1038/nrmicro.2017.126.

[3] Sun L, Zhang H, Fang T, Wang Y, Liu Y, Wang X, Dong Q. A review of the biofilm formation and transfer of *Listeria monocytogenes* in the food environment and prevention and control measures for it. Food Sci (N Y) 2021;42(13):289–99.

[4] Hu L, Dong Q, Xia Y, Zhang S, Yang J, Wang Z, Liu Y. Advances on the formation and regulation mechanism of *Listeria monocytogenes* biofilm. Food Ferment Ind 2021;47(8):276–82.

[5] Lu L, Hu W, Tian Z, Yuan D, Yi G, Zhou Y, Cheng Q, Zhu J, Li M. Developing natural products as potential anti-biofilm agents. Chin Med 2019;14.

[6] Wang T, Cornel EJ, Li C, Du J. Drug delivery approaches for enhanced antibiofilm therapy. J Contr Release 2023;353:350–65.

[7] Morita T, Fukuoka T, Imura T, Kitamoto D. Production of mannosylerythritol lipids and their application in cosmetics. Appl Microbiol Biotechnol 2013;97(11):4691–700. https://doi.org/10.1007/s00253-013-4858-1.

[8] de Andrade CJ, de Andrade LM, Rocco SA, Sforca ML, Pastore GM, Jauregi P. A novel approach for the production and purification of mannosylerythritol lipids (MEL) by *Pseudozyma tsukubaensis* using cassava wastewater as substrate. Separ Purif Technol 2017;180:157–67. https://doi.org/10.1016/j.seppur.2017.02.045.

[9] Fukuoka T, Morita T, Konishi M, Imura T, Kitamoto D. Characterization of new types of mannosylerythritol lipids as biosurfactants produced from soybean oil by a basidiomycetous yeast, *Pseudozyma shanxiensis*. J Oleo Sci 2007;56(8):435–42.

[10] Jezierska S, Claus S, Van Bogaert I. Yeast glycolipid biosurfactants. FEBS Lett 2018;592(8):1312–29. https://doi.org/10.1002/1873-3468.12888.

[11] Silva Coelho AL, Feuser PE, Mattar Carciofi BA, de Andrade CJ, de Oliveira D. Mannosylerythritol lipids: antimicrobial and biomedical properties. Appl Microbiol Biotechnol 2020;104(6):2297–318. https://doi.org/10.1007/s00253-020-10354-z.

[12] Fukuoka T, Morita T, Konishi M, Imura T, Sakai H, Kitamoto D. Structural characterization and surface-active properties of a new glycolipid biosurfactant, mono-acylated mannosylerythritol lipid, produced from glucose by *Pseudozyma antarctica*. Appl Microbiol Biotechnol 2007;76(4):801–10. https://doi.org/10.1007/s00253-007-1051-4.

[13] Kitamoto D, Isoda H, Nakahara T. Functions and potential applications of glycolipid biosurfactants - from energy-saving materials to gene delivery carriers. J Biosci Bioeng 2002;94(3):187–201. https://doi.org/10.1263/jbb.94.187.

[14] Kitamoto D, Yanagishita H, Shinbo T, Nakane T, Kamisawa C, Nakahara T. Surface-active properties and antimicrobial activities of mannosylerythritol lipids as biosurfactants produced by *Candida-Antarctica*. J Biotechnol 1993;29(1–2):91–6. https://doi.org/10.1016/0168-1656(93)90042-l.

[15] Lencova S, Zdenkova K, Demnerova K, Stiborova H. *Short communication*: antibacterial and antibiofilm effect of natural substances and their mixtures over *Listeria monocytogenes, Staphylococcus aureus* and *Escherichia coli*. LWT–Food Sci Technol 2022;154.

[16] Fan L, Li H, Niu Y, Chen Q. Characterization and inducing melanoma cell apoptosis activity of mannosylerythritol lipids-a produced from *Pseudozyma aphidis*. PLoS One 2016;11(2). https://doi.org/10.1371/journal.pone.0148198.

[17] Felipe V, Laura Breser M, Paola Bohl L, Rodrigues da Silva E, Andrea Morgante C, Graciela Correa S, Porporatto C. Chitosan disrupts biofilm formation and promotes biofilm eradication in *Staphylococcus* species isolated from bovine mastitis. Int J Biol Macromol 2019;126:60–7. https://doi.org/10.1016/j.ijbiomac.2018.12.159.

[18] Cui H, Zhang C, Li C, Lin L. Antimicrobial mechanism of clove oil on *Listeria monocytogenes*. Food Control 2018;94:140–6. https://doi.org/10.1016/j.foodcont.2018.07.007.

[19] Sabaeifard P, Abdi-Ali A, Soudi MR, Dinarvand R. Optimization of tetrazolium salt assay for *Pseudomonas aeruginosa* biofilm using microtiter plate method. J Microbiol Methods 2014;105:134–40. https://doi.org/10.1016/j.mimet.2014.07.024.

[20] Liu XY, Shu Q, Chen QH, Pang XX, Wu YS, Zhou WY, Zhang XL. Antibacterial efficacy and mechanism of mannosylerythritol lipids-a on *Listeria monocytogenes*. Molecules 2020;25(20). https://doi.org/10.3390/molecules25204857.

[21] Shu Q, Wei TY, Lu HY, Niu YW, Chen QH. Mannosylerythritol lipids: dual inhibitory modes against *Staphylococcus aureus* through membrane-mediated apoptosis and biofilm disruption. Appl Microbiol Biotechnol 2020;104(11):5053–64. https://doi.org/10.1007/s00253-020-10561-8.

[22] Ma T, Ouyang T, Ouyang HS, Chen FW, Peng ZY, Chen XR, Ren LZ. Porcine circovirus 2 proliferation can be enhanced by stably expressing porcine *IL-2* gene in PK-15 cell. Virus Res 2017;227:143–9. https://doi.org/10.1016/j.virusres.2016.10.006.

[23] Rashid MH, Kornberg A. Inorganic polyphosphate is needed for swimming, swarming, and twitching motilities of *Pseudomonas aeruginosa*. Proc Natl Acad Sci USA 2000;97(9):4885–90. https://doi.org/10.1073/pnas.060030097.

[24] Abhinav U, Indu U, Anup K-J, Kumar V. Antibiofilm effect of plant derived antimicrobials on *Listeria monocytogenes*. Food Microbiol 2013;36(1):79–89.

[25] Cui H, Zhang C, Li C, Lin L. Inhibition of *Escherichia coli* O157:H7 biofilm on vegetable surface by solid liposomes of clove oil. LWT–Food Sci Technol 2020;117. https://doi.org/10.1016/j.lwt.2019.108656.

[26] Bellich B, Lagatolla C, Tossi A, Benincasa M, Cescutti P, Rizzo R. Influence of bacterial biofilm polysaccharide structure on interactions with antimicrobial peptides: a study on *Klebsiella pneumoniae*. Int J Mol Sci 2018;19(6). https://doi.org/10.3390/ijms19061685.

[27] Liu J, Yang L, Kjellerup BV, Xu Z. Viable but nonculturable (VBNC) state, an underestimated and controversial microbial survival strategy. Trends Microbiol 2023;31(10):1013–23.

[28] Flemming H-C, Wingender J. The biofilm matrix. Nat Rev Microbiol 2010;8(9):623–33. https://doi.org/10.1038/nrmicro2415.

[29] Han Q, Song X, Zhang Z, Fu J, Wang X, Malakar PK, Zhao Y. Removal of foodborne pathogen biofilms by acidic electrolyzed water. Front Microbiol 2017;8. https://doi.org/10.3389/fmicb.2017.00988.

[30] Tan L, Zhao F, Han Q, Zhao A, Malakar PK, Liu H, Zhao Y. High correlation between structure development and chemical variation during biofilm formation by *Vibrio parahaemolyticus*. Front Microbiol 2018;9. https://doi.org/10.3389/fmicb.2018.01881.

[31] Fan Y, Qiao J, Lu Z, Fen Z, Tao Y, Lv F, Bie X. Influence of different factors on biofilm formation of *Listeria monocytogenes* and the regulation of *cheY* gene. Food Res Int 2020;137. https://doi.org/10.1016/j.foodres.2020.109405.

[32] Lemon KP, Higgins DE, Kolter R. Flagellar motility is critical for *Listeria monocytogenes* biofilm formation. J Bacteriol 2007;189(12):4418–24. https://doi.org/10.1128/jb.01967-06.

[33] Wang F, Deng L, Huang F, Wang Z, Lu Q, Xu C. Flagellar motility is critical for *Salmonella* enterica serovar typhimurium biofilm development. Front Microbiol 2020;11. https://doi.org/10.3389/fmicb.2020.01695.

[34] Ma Y, Shi Q, He Q, Chen G. Metabolomic insights into the inhibition mechanism of methyl N-methylanthranilate: a novel quorum sensing inhibitor and antibiofilm agent against *Pseudomonas aeruginosa*. Int J Food Microbiol 2021;358. https://doi.org/10.1016/j.ijfoodmicro.2021.109402.

[35] Wang N, Gao J, Yuan L, Jin Y, He G. Metabolomics profiling during biofilm development of *Bacillus licheniformis* isolated from milk powder. Int J Food Microbiol 2021;337. https://doi.org/10.1016/j.ijfoodmicro.2020.108939.

[36] Murata N, Los DA. Membrane fluidity and temperature perception. Plant Physiol 1997;115(3):875–9. https://doi.org/10.1104/pp.115.3.875.

[37] Maceyka M, Payne SG, Milstien S, Spiegel S. Sphingosine kinase, sphingosine-1-phosphate, and apoptosis. Biochim Biophys Acta Mol Cell Biol Lipids 2002;1585(2–3):193–201. https://doi.org/10.1016/s1388-1981(02)00341-4.

[38] Wilhelm F, Hirrlinger J. Multifunctional roles of NAD(+) and NADH in astrocytes. Neurochem Res 2012;37(11):2317–25. https://doi.org/10.1007/s11064-012-0760-y.

[39] Oloketuyi SF, Khan F. Inhibition strategies of *Listeria monocytogenes* biofilms current knowledge and future outlooks. J Basic Microbiol 2017;57(9):728–43. https://doi.org/10.1002/jobm.201700071.